Accepted Manuscript

A novel NAE/UAE dual inhibitor LP0040 blocks neddylation and ubiquitination leading to growth inhibition and apoptosis of cancer cells

Peng Lu, Yahui Guo, Lijuan Zhu, Yineng Xia, Yuejiao Zhong, Yubin Wang

PII: S0223-5234(18)30437-9

DOI: 10.1016/j.ejmech.2018.05.027

Reference: EJMECH 10438

To appear in: *European Journal of Medicinal Chemistry*

Received Date: 27 December 2017

Revised Date: 3 May 2018

Accepted Date: 17 May 2018

Please cite this article as: P. Lu, Y. Guo, L. Zhu, Y. Xia, Y. Zhong, Y. Wang, A novel NAE/UAE dual inhibitor LP0040 blocks neddylation and ubiquitination leading to growth inhibition and apoptosis of cancer cells, *European Journal of Medicinal Chemistry* (2018), doi: 10.1016/j.ejmech.2018.05.027.

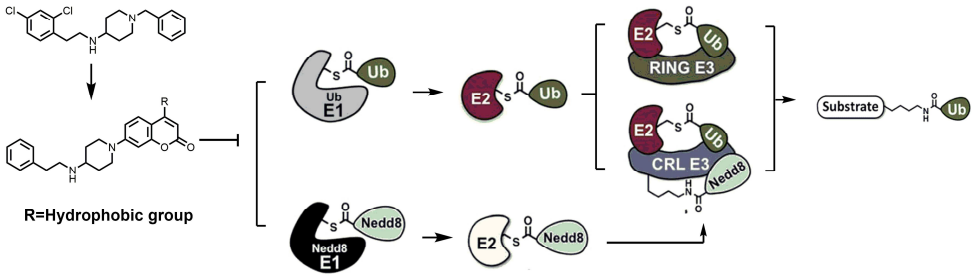

A Novel NAE/UAE Dual Inhibitor LP0040 Blocks Neddylation and Ubiquitination Leading to Growth Inhibition and Apoptosis of Cancer Cells

Peng Lu [1], Yahui Guo [2], Lijuan Zhu [1], Yineng Xia [1], Yuejiao Zhong [3], Yubin Wang [1*].

[1] School of Pharmaceutical Sciences, Nanjing Tech University, No. 5 Xinmofan Road, Nanjing 210009, People's Republic of China.

[2] Department of pharmaceutical science, China Pharmaceutical University, No. 24 Tongjia Xiang, Nanjing 210009, People's Republic of China.

[3] The Affiliated Cancer Hospital of Nanjing Medical University, No. 42 Baiziting, Nanjing 210009, People's Republic of China.

Keywords: NEDD8 activating enzyme, ubiquitin activating enzyme, dual inhibitor, apoptosis, drug discovery.

Abstract

NEDD8 activating enzyme (NAE) plays an important role in regulating intracellular proteins with key parts in a broad array of cellular functions. On the basis of previously work, a series of 2H-chromen-2-one based NAE inhibitors were designed and synthesized. Through enzyme-based and cell-based assays, **LP0040** was identified as a non-nucleoside NAE/UAE dual inhibitor. It could inhibit NAE/UAE activities and downregulated degradations of related substrates in AGS cells, promoting apoptosis in low micromole concentrations. **LP0040** possessed anti-proliferation activities with IC_{50} values of 0.76 – 3.29 μM against multiple human cancer lines and had synergistic effect with bortezomib. Thus **LP0040** represented valuable starting points for future development of NAE/UAE dual inhibitors.

1. Introduction

The ubiquitin-proteasome system (UPS) is responsible for regulated degradation of intracellular proteins with important roles in a broad array of cellular functions [1]. In UPS, proteins labelled by ubiquitin (Ub) will be recognized and degraded by proteasome. Proteasome inhibitor bortezomib (Velcade) which targets the proteasome is approved for the treatment of multiple myeloma and mantle cell lymphoma [2, 3]. The successful clinical application of bortezomib raises the question whether inhibitors of other enzymes that modulate UPS activity can lead to the development of new anti-cancer drugs. Ubiquitin-like protein (Ubl) conjugation pathways, including NEDD8 and SUMO, have also been identified as key players in the protein degradation process. Targeting Ubl conjugation pathways has been considered to be more advantageous for therapeutic intervention, as Ubl pathways have fewer downstream conjugation targets and a smaller subset of proteins will be affected.

Ub and Ubls typically modulate protein function following covalent attachment to substrate proteins by E1, E2 and E3 cascade catalyzations. The Ub pathway is representative of those processes and is shown in Fig. 1. In the first step, Ubiquitin-activating enzyme (UAE, E1) consumes ATP to form Ub-AMP, which is a rate-limiting step. Then, Ub is passed to ubiquitin conjugating enzymes (E2) through a transthiolation reaction. The Ub-E2 then binds an ubiquitin ligase (E3), and Ub is finally transferred to a lysine residue on its substrate protein. Ubl pathways are similar to the ubiquitin pathway. Ubls are transferred to their substrates through cascade catalyzations which are catalyzed by corresponding E1, E2 and E3.

The covalent attachment of NEDD8, termed neddylation, is a reversible and multi-step process analogous to ubiquitination. Neddylation plays a crucial role in the assembly and function of the largest family of E3 ubiquitin ligases, the cullin ring ligases (CRL). Modification of the cullin-RING ubiquitin E3 ligases (CRLs) by NEDD8 is known to be essential for the CRL-mediated ubiquitination of downstream targets in the UPS, which is critically involved in protein homeostasis [4-6]. Other substrates of neddylation include the mouse double minute 2 (MDM2) oncogene product [7], the p53 tumor suppressor protein [7, 8], the von Hippel-Lindau protein (pVHL) [9], the breast cancer associated protein 3 (BCA3) [10] , and the estrogen receptor-R. (ERR) [11]. As the NEDD8 pathway controls the degradation of a specific subset of proteins regulated by CRLs, it has been considered as a more specific target compared to the UPS protein degradation pathway. Because NEDD8 activating

enzyme (NAE) is involved in the rate-limiting step of neddylation, inhibition of NAE can modulate the rate of ubiquitination and subsequent degradation of proteins which are regulated by CRLs. NAE has recently emerged as a new target for the treatment of cancer [12-14].

MLN4924 (**1**, shown in **Fig. 2**) is the first reported NAE inhibitor. Treating cancer cells with MLN4924 led to varieties of biological effects such as checkpoint activation, DNA re-replication and apoptosis in multiple cancer cell lines [12, 15]. MLN4924, whose Phase 1 clinical trials is completed, has been shown to be effective for the treatment of both solid (colon, lung) and hematological (myeloma, lymphoma) human cancers. However, treatment-emergent heterozygous mutations of NAE and resistance to MLN4924 have already been identified in preclinical studies [16-18]. In recent years, some moderate NAE inhibitors has been reported, such as natural product-like compounds **2–3**, metal complex **4** and ene-rhodanine analogue **5** (**Fig. 2**), but while there still were some shortages about potency and druglike physical properties in those compounds [19-22]. Besides that, ABP A3 which was a nucleoside analogue (**6**, shown in **Fig. 2**) was reported as an NAE and UAE dual inhibitor [23]. ABP A3 would form Ub-ABP A3 and NEDD8-ABP A3 catalyzed by UAE and NAE respectively and subsequently inhibited NAE and UAE activities. Besides that, some other NAE inhibitors were also reported recently[24, 25]. In our previous work, **M22** (**7**, shown in **Fig. 2**) was identified as a novel reversible inhibitor of NAE through high-throughput virtual screening from a compound library containing 50000 small molecular entities [26]. **M22** is reversible for NAE, inhibits multiple cancer cell lines with IC_{50} values in low micromolar range, induces apoptosis in A549 cells, and produces tumor inhibition in AGS xenografts in nude mice. In this article, **LP0040** is a non-nucleoside NAE and UAE dual inhibitor that was identified through rational drug design on the basis of **M22**. By verification, **LP0040** exhibited proliferation inhibition against multiple cell lines and induced apoptosis in AGS cells (gastric adenocarcinoma cells). Furthermore, synergistic effect on anti-proliferation between **LP0040** and bortezomib was also observed in this study.

2. Results and discussion

2.1. Molecular modeling and drug design

APPBP1-UBA3-NEDD8-ATP complex (PDB ID: 1R4N) was used for molecular modeling in our previous work. **M22** was docked into the ATP binding pocket, and molecular modeling results showed that the 2, 4-dichloro-1-phenethyl group of **M22** was predicted to map onto the phosphate groups of ATP, and that benzyl group was forecasted to be located in the pocket where the adenine of ATP

occupied. **M22** was estimated to form one H-bond between the carboxyl group of Gly176 and the secondary amine of **M22**. Additionally, 2, 4-dichlorophenyl group was estimated to have cation-π interactions with Arg90 and Arg15. Herein, the replacement of benzyl group of **M22** by adenine analogous structure was considered to improve NAE inhibitory activity. Novobiocin was a DNA gyrase and DNA topoisomerase IV dual inhibitor, whose 2H-chromen-2-one structure mapped onto the adenine of ATP according to co-crystals of novobiocin with those two enzymes (PDB ID: 4URO, 1S14)[27, 28]. Therefore, 7-(4-(phenethylamino)piperidin-1-yl)-2H-chromen-2-one (**8**, shown in **Fig. 3**) was designed, with benzyl group of **M22** replaced by 2H-chromen-2-one. According to docking results (**Fig. 3**), phenenyl group was estimated to have cation-π interactions with Arg90 and one H-bond was formed between the carboxyl group of Gly176 and the secondary amine. More importantly, a new H-bond was formed between the carbonyl in 2H-chromen-2-one and the backbone of Ile127.

The docking model was investigated carefully, and a hydrophobic region (in UBA3 subunit) which was formed by Ile127, Ile149, Ala150 and Trp153was found behind the 4-position of 2H-chromen-2-one. In the co-crystal of NAE-NEDD8-MLN4924 (PDB ID: 3GZN), 2,3-dihydro-1H-inden-1-yl group was located in the hydrophobic region mentioned above. Therefore, hydrophobic substituents were introduced to 4-position of 2H-chromen-2-one to occupy the hydrophobic region.

Biaryl structures, with rotatable bond, suitable rigidity, volume and shape, are fit for binding with proteins and are considered as privileged structures in anti-tumor drugs[29]. For the reason above, hydrophilic and hydrophobic aryl rings were introduced on the 4 position of 2H-chromen-2-one (**9-14,** shown in **Fig. 4A**). As shown in **Table 1**, 2H-chromen-2-one derivatives with phenyl substituents (**9-12**) increased anti-proliferation activities against A549 (lung cancer), K562 (chronic myelogenous leukemia), HCT-116 (colorectal carcinoma), SKOV-3 (ovarian cancer), BxPC-3 (pancreatic cancer) and AGS (gastric cancer) cells, comparing with **M22**. Cancer cells used in this study were neddylation up-regulated (A549) or MLN4924 sensitive [2, 12-14, 30]. Furthermore, compound **11** could inhibit proliferation of AGS cells with the lowest IC_{50} value of 0.76 μM. However, uracil (**13**) and 1,2,3-1H-triazole (**14**) substituted derivatives could not inhibit proliferation of tested cells even at the concentration of 30 μM. Those results suggested that 4-hydrophobic substituents would favor inhibition activities, but 4- hydrophilic substituents would not.

In this study, ethynyl group was introduced as a linker connecting 2H-chromen-2-one with rings,

owing to its hydrophobicity and linear structure. So compounds **15-18** (shown in **Fig. 4A**) were designed, synthesized and evaluated. As shown in **Table 1**, those 4-ethynyl substituted derivatives exhibited increased anti-proliferation activities, indicating that introducing ethynyl groups on 4-position of 2H-chromen-2-one would also contribute to the increasing of anti-proliferation activity.

One of the drawbacks of 2H-chromen-2-ones described earlier is the red blood cell hemolysis. The hemolytic activities of **9, 10, 11**, **12**, **15, 16**, **17** and **18** on rabbit red blood cells were assessed to gain further insight into the potential toxic effects of the tested compounds. As shown in **Fig. 4B**, there was no apparent sign of toxicity (<10% at 100 μM) to erythrocytes for **11**, **16**, and **17** at the concentration of 100 μM, compared to MLN4924 (5.80% at 100 μM) In addition, Log P values of compound **9, 10, 11**, **12**, **15, 16**, **17** and **18** were also measured, and Log P value of each compound was between 1 and 5 (shown in **Fig. 4C**).

Then, **11** was chose to investigate its toxicity against normal cells. In this study, HEK293T, HUVEC and L-02 cells were used and LC_{50} values of **11** were respectively 12.93 μM, 10.69 μM and 13.54 μM (shown in **Table 2**), which were about 14-18 times than IC_{50} values against AGS cells. However, bortezomib showed non-selectivity against cancer cells and normal cells. Considering that NAE was widely expressed in non-cancer cells at a low level, NAE inhibitors would have some effect on non-cancer cells at high concentrations. The difference between the anti-proliferation activities of **11** against AGS cells and tested normal cells suggested that proliferation inhibition of **11** against AGS cells might be induced by NAE inhibition rather than general toxicity. Furthermore, those results indicated that NAE inhibitor might target cancer cells more selectively over normal cells.

With the lowest IC_{50} value against AGS cells and moderate selectivity to normal cells, **11** (**LP0040**) was selected for further validation.

2.2. LP0040 inhibited NAE activity in enzyme-based assay

A dose-response experiment was performed using an enzymatic assay which measured the level of NAE-mediated formation of the Ubc12-NEDD8 (Ubc12 is one of E2s for NEDD8 conjugation) thioester product in a cell-free system. Decreased level of Ubc12-NEDD8 conjugation indicates the inhibition of NAE. Recombinant human NAE was incubated with NEDD8, Ubc12 and ATP in the presence of **LP0040** for 1h. Then levels of Ubc12-NEDD8 thioester product were detected by western blot. A concentration-dependent reduction of the intensity of Ubc12-NEDD8 bands was observed and formation of Ubc12-NEDD8 was evidently inhibited at 0.37 μM (**Fig. 5A** and Supplementary **Fig. S1A**),

indicating that compound **LP0040** was an effective NAE inhibitor.

2.3. LP0040 inhibited NAE activity in cell-based assay

To validate whether **LP0040** could inhibit NAE in AGS cells, AGS cells which were treated with **LP0040** under 0 – 90 μM for 24 h were lysed and protein extracts were analyzed by western blot. The NEDD8 combined Uba3 was noticeably decreased in a concentration-dependent manner, as well as the decrease of Ubc12-NEDD8 and Cullins-NEDD8 (**Fig. 5B** and Supplementary **Fig. S1B**), indicating that NAE activity was inhibited and that neddylation was suppressed by **LP0040**. Inhibition of NAE activity results in the inactivation of CRLs, leading to a decreased degradation of proteins which are mediated by CRLs. As shown in **Fig. 5B** and **Fig. S1C**, treatment of AGS cells with **LP0040** for 24 h resulted in a reciprocal increase in the abundance of known CRL substrates CDT1, p27 and NRF2, suggesting that **LP0040** could stabilize CRL substrates through suppressing neddylation. However, **13** which was selected as a negative control in this assay was not able to inhibit NAE activity or block neddylation of CRLs (**Fig. 5D** and Supplementary **Fig. S1D**). From those data, **LP0040** was considered to suppress NAE activity and to downregulate neddylation in vitro.

2.4. Selectivity of LP0040

As NAE was homologous to Ub and Ubl E1s, the selectivity profile of **LP0040** for NAE was also investigated in cell-based assays evaluating levels of E2-UBL thioester products by western blot. As shown in **Fig. 5C**, formation of those Ubc9-SUMO and USE1-Ub (Ubc9 and Use1 are E2 enzymes that participate in the conjugation cascade for SUMO and FAT10 labeling, respectively) were almost not suppressed at different concentrations of **LP0040**, while neddylation was blocked by **LP0040** at those concentrations, which illustrated that **LP0040** had no inhibition on SAE and Uba6. However, **LP0040** showed a degree of inhibitory activity on UAE, so that **LP0040** might be an NAE/UAE dual inhibitor.

Since 2H-chromen-2-one are known as promiscuous binders to ATP binding pocket, **LP0040** was also submitted to a selectivity screen against a panel of 13 kinases. As shown in **Table 3**, **LP0040** showed less than 15 % inhibition against tested kinases at 30 μM, indicating that **LP0040** might have little effect to other kinases.

2.5. NAE and UAE Dual Inhibition by LP0040

To test whether **LP0040** was an UAE inhibitor, an enzyme based assay was also conducted. Similar to NAE inhibition assay, UAE was incubated with Ub, Ubc10 and ATP in the presence of **LP0040** for 1h. Levels of Ubc10-Ub thioester product were detected by western blot. As shown in **Fig. 5A** and

Supplementary **Fig. S1A**, **LP0040** also suppressed Ubc10-Ub formation, suggesting that **LP0040** was an NAE/UAE dual inhibitor.

2.6. Apoptosis Induced by LP0040 In AGS Cells

Flow cytometic analysis showed that apoptotic cells appeared with a dose-dependent pattern in **LP0040**-treated AGS cells when the cells were double labelled with annexin-V-FITC and PI (**Fig. 6**). After treatment with **LP0040**, the apoptotic rates (Annexin V^+) of AGS cells were increased to 83.44% of total cells (10 μM, 12 h) whereas only few cells were observed as apoptotic cells in the control group. Besides that, necrotic rates (PI+/Annexin V-) of AGS cells were always below 10%. Caspase-3 is a cytosolic protein that is activated by proteolytic cleavage. It is one of the key factors in the apoptotic pathway. The inactive 32 kDa proenzyme can be cleaved into 20 kDa (p20) and 11 kDa (p11) active subunits, which can lead to cell apoptosis. In this study, we examined the promotion effects of **LP0040** on the activation of caspase-3 in AGS cells after 24 h treatment. As shown in **Fig. 5B** immunoblot analysis indicated that **LP0040** treatment increased the expression of cleaved caspase 3. Taken together, these results suggested that treatment of **LP0040** promoted cell apoptosis in AGS through activating caspase 3.

2.7. G1 Arrest and Apoptosis Induced by LP0040

To further explore whether growth inhibition and apoptosis induced by **LP0040** was associated with regulation of the cell cycle, DNA content of cell nuclei was detected by flow cytometry. The effects of **LP0040** on AGS cell cycle distribution were shown in **Fig. 7A-7B**. With the percentage of G1 phase increased from 22.82% to 48.88%, AGS cell cycle was arrested in G1, treated with 4 μM **LP0040**. Furthermore, treating AGS cells with 4 μM **LP0040**, sub-G1 cells were detected at 24 h, indicating that **LP0040** could induce apoptosis.

2.8. Synergistic Effect of LP0040 with Bortezomib

Because NEDD8 pathway locates on the upstream of UPS, **LP0040** may have synergistic effects with bortezomib which is a selective inhibitor of 26S proteasome on the downstream of UPS. To verify the effect of combination of **LP0040** and bortezomib on AGS cells, Jin equation (the modified Burgi formula, shown below) whose concept was universally accepted in pharmacology was employed [31, 32]. In Jin equation, the q values presenting < 0.85, 0.85–1.25, 1.25–2 and > 2 suggest antagonism, simple addition, synergism and apparent synergism respectively. Inhibition efficiency of drug alone and drug combination on AGS cells' growth at 48 h after drug introduction were measured and q

values for every drug combination at different concentrations were calculated. Results are shown in **Fig. 7C** and **Table 4**. Synergistic effect on anti-proliferation was observed in those drug combinations as follows: 10 nM BTZ with 1 μM LP0040, 10 nM BTZ with 1.25 μM LP0040 and 10 nM BTZ with 1.5 μM LP0040. In addition, apparent synergism was noticed in drug combinations, such as 1.25 μM LP0040 with 5 nM or 7 nM BTZ.

$$q = \frac{E_{\mathbf{LP0040}+BTZ}}{E_{\mathbf{LP0040}} + E_{BTZ} - E_{\mathbf{LP0040}} \times E_{BTZ}}$$

Where $E_{\mathbf{LP0040}}$, E_{BTZ} and $E_{\mathbf{LP0040}+BTZ}$ are the inhibition rates of **LP0040**, bortezomib, and combination of **LP0040** and bortezomib, respectively.

Proteasome inhibitors bortezomib and carfilzomib are clinically used as first-in-line treatments for multiple myeloma now, and show clear clinical efficacy. However, these agents have not found use as therapeutic agents to treat solid tumors. In some cases, proteasome inhibitors also have shown limited clinical efficacy in treating multiple myeloma [33-35]. These limited responses are in part due to the alternative degradation of misfolded proteins via the aggresomal pathway. Therefore, new approaches to UPS are urgently needed. Inhibitors of UAE and NAE activating enzyme are potential therapeutic agents. Pharmacological dual inhibition of UAE and NAE inhibits ubiquitin conjugation, resulting in protein degradation suppression. This paper reported the discovery of **LP0040**, a non-nucleoside NAE/UAE dual inhibitor, which inhibited both NEDD8-independent and NEDD8-dependent ubiquitin conjugation and protein degradation. Then **LP0040** was used to validate the therapeutic potential of the UPS to treat solid tumor through using AGS cells as a model system.

On the basis of **M22** which was a new class of NAE inhibitor, a series of 4-substituted 2H-chromen-2-one derivatives were designed and synthesized. In this study, the modification strategy used was similar to a previous work reported by J.L. Lukkarila [30]. However, rigid groups instead of flexible groups were introduced to occupy the back hydrophobic pocket, which might improve selectivity. Through anti-proliferation assay, 4-hydrophobic substituents was found favor activities of 2H-chromen-2-one derivatives, and that 4- hydrophilic substituents was not. **LP0040** could inhibit proliferation of AGS cells with evidently inhibition against NAE. Meanwhile, compound **13** whose 4-position of 2H-chromen-2-one was substituted by a hydrophilic group almost have no effect on NAE activity or AGS proliferation. Those results indicated necessity of hydrophobic substituent on the 4-position of 2H-chromen-2-one for NAE inhibition. Investigating the docking model carefully, a

hydrophobic region was found locating behind the 4-position of 2H-chromen-2-one. The docking model coincided with experiment results, suggesting that the docking model could be used as a prediction model for molecular modification.

LP0040 showed the lowest IC_{50} value against AGS cells. Treatment of AGS cells with **LP0040** for 24 h induced a dose-dependent decrease of NEDD8 and Ub conjugations, resulting in a reciprocal increase in the abundance of the known CRL substrates CDT1, NRF2 and p27. When the concentration of **LP0040** was 8 μM, NEDD8 conjugation was almost completely inhibited. On contrast, CRL substrates were accumulated noticeably and cleaved caspase 3 was observed at 8 μM of **LP0040**. Correspondingly, Anexin V-positive cells were detected at 8 μM of **LP0040**. Therefore, proliferation inhibition and apoptosis were induced by UAE/NAE dual suppression of **LP0040**, but not cytotoxicity. Although expected selectivity was not achieved, an UAE/NAE dual inhibitor was identified. Furthermore, **LP0040** was proved to inhibit proliferation of multiple cell lines and have synergistic action on anti-proliferation activity with bortezomib. Thus **LP0040** might improve the therapeutic efficacy of bortezomib in solid tumors in the future.

3. Conclusion

The identification of **LP0040** and related 2H-chromen-2-ones as UAE/NAE inhibitors represents an important step forward in developing leads for preclinical evaluation of inhibitors of UAE/NAE in cancer and potentially other diseases. **LP0040** increases the level of a cell cycle inhibitor, activates caspase 3, and induces cell apoptosis. All of these are desirable effects for a cancer therapeutic. However, inhibitors of UAE/NAE are considered to induce undesirable side effects on protein dynamics as proteasome inhibitors. In this paper, a simple structure-activity relationship (SAR) study was conducted, and a more detailed SAR investigation was needed to develop leads for preclinical evaluation of inhibitors of UAE/NAE in cancer and potentially other diseases. Further investigations of the pharmacological properties of **LP0040** in vitro and in vivo will also be reported in the near future.**4.**

4. Experiment sections

4.1 Chemistry

4.1.1 General procedures for the synthesis of target compounds

The synthetic strategy used to prepare the target compounds **9**-**18** is outlined in Scheme 1-2. The key intermediate **28** was synthesized from phenethylamine (**19**) and 4-bromo-2-hydroxyacetophenone (**23**) as start materials. Intermediate **20** was made from **19** and N-benzyl-4-piperidone through Borch

reduction. Compound **21** was obtained by protection of **20**'s secondary amine, which was followed by Pd/C catalytic hydrogenation to provide intermediate **22**. In present of NaH, start material **23** reacted with dimethyl carbonate to provide compound **24** by one-pot synthesis. Intermediate **25** was obtained by protection of hydroxyl group in compound **24**. Through Buchwald–Hartwig coupling reaction, compound **26** was synthesized from intermediate **22** and **25**. With Pd/C catalytic hydrogenation of compound **26**, compound **27** was obtained. Then compound **27** reacted with trifluoromethanesulfonic anhydride to get key intermediate **28**. From intermediate **28,** Target compounds **9**-**13** could be achieved through Suzuki-Miyaura coupling reaction and deprotection of Boc, while compounds **15-18** would be provided through Sonogashira coupling reaction and deprotection of Boc. Target compound **14** was synthesized from intermediate **28** through Sonogashira coupling with Trimethylsilylacetylene, addition reaction with trimethylsilylacetylene, and deprotection of Trimethylsilyl group and Boc group.

4.1.2 Synthetic method

Synthetic method is detailedly described in supplementary methods.

4.2. Tested compounds

Bortizomib (B48966) was provided by Bepharm (Shanghai, China). Tested 2H-chromen-2-one derivatives were synthesized according to **Scheme 1–2**. All synthesized target compounds were characterized by ^{1}H NMR (Supplementary **Fig. S2–Fig. S21**), ^{13}C NMR (Supplementary **Fig. S22–Fig. S31**) and HPLC (Supplementary **Fig. S32–Fig. S41**). Purity of all tested compounds was all over 95%.

4.3. Cell Lines and Culture Conditions

The tumor cell lines used in this study were obtained from the American Type Culture Collection (ATCC), unless specified otherwise. K562 (provided by professor Hai Qian, China Pharmaceutical University), BxPC-3 (CRL-1687), and A549 (CCL-185) cells were grown in RPMI 1640 (Wisent)/10% (v/v) fetal bovine serum (FBS, Wisent). AGS (CL-0022, from Procell) cells were cultured in Ham's F12 medium (Wisent)/10% (v/v) FBS. HCT-116 (CCL-247) and SKOV-3 (HTB-77) were cultured in DMEM medium (Wisent)/10% (v/v) FBS. All cells were cultured at 37 ˚C with 5% CO_2. All cell lines were obtained between 2010 and 2016 and kept in culture up to 15 to 20 passages, but not longer than 6 months. All cell lines were authenticated by the suppliers using short tandem repeat (STR) analysis.

4.4. Antiproliferation assay

Cell counting kit-8 (CCK-8, Dojindo) was used to evaluate the proliferation of cultured cells [36, 37]. Cancer cells (K562, BxPC-3, A549, HCT-116, SKOV-3 and AGS) were prepared and diluted to a

concentration of 6×10^4 cells/mL. 100 μL of the cell suspension was seeded in each well of 96-well plates, totaling 6×10^3 cells/well. After 12 h incubation at 37 ˚C in 5% CO_2, the medium in the plates was replaced by 150 μL medium containing serial dilutions of compounds. Bortizomib was used as a positive control. Following 48 h culture, 10 μL CCK-8 was added to each well and cells were incubated for another 4 h. The light absorption value (OD) of each well was measured at 450 nm. The experiment was repeated 3 times. IC_{50} values were calculated from the inhibition curves by normalized nonlinear regression analysis using GraphPad Prism 5 software.

4.5. Enzyme based NAE activity assay

This assay was performed using the NEDD8 conjugation initiation kit (K-800, R&D) according to the instructions of the manufacturer. 2 μL NAE (2.5 μM), 2 μL NEDD8 (250 μM), 2 μL Ubc12 (50 μM, Ubc12 is the E2 enzyme that participate in the conjuation cascade for Nedd8 labeling), 2 μL reaction buffer and 10 μL water solution of **LP0040** (0 μM, 0.12μM, 3.7 μM, 1.11 μM, 3.33 μM, 10 μM) were added into 100 μL reaction tubes in order. Reaction solutions were incubated at 37 ˚C for 10 min. The reaction was initiated by the addition of 2 μL Mg^{2+}/ATP solution (10 mM), and the mixture was incubated at 37 ˚C for 60 min. In negative control group, 2 μL ddH_2O was added instead of ATP solution. The reaction was quenched by the addition of 2 μL EDTA (1 M), and protein samples were electrophoresed under non-reducing conditions on a 15% SDS-PAGE gel. Ubc12-NEDD8 levels were determined by western blot analysis.

4.6. Enzyme based UAE activity assay

This assay was performed using the ubiquitin conjugation initiation kit (K-995, R&D) according to the instructions of the manufacturer. 2 μL UAE (2.5 μM), 2 μL Ub (250 μM), 2 μL Ubc10 (50 μM, Ubc10 is the E2 enzyme that participate in the conjuation cascade for ubiquitin labeling), 2 μL reaction buffer and 10 μL water solution of **LP0040** (0 μM, 0.12μM, 3.7 μM, 1.11 μM, 3.33 μM, 10 μM) were added into 100 μL reaction tubes in order. Reaction solutions were incubated at 37 ˚C for 10 min. The reaction was initiated by the addition of 2 μL Mg^{2+}/ATP solution (10 mM), and the mixture was incubated at 37 ˚C for 60 min. In negative control group, 2 μL ddH_2O was added instead of ATP solution. The reaction was quenched by the addition of 2 μL EDTA (1 M), and protein samples were electrophoresed under non-reducing conditions on a 15% SDS-PAGE gel. Ubc10-Ub levels were determined by western blot analysis.

4.7. Cell based NAE activity assay

AGS cells were exposed to the indicated concentrations of **LP0040** (2 μM, 4 μM, 6 μM, 8 μM, 10 μM) or 0.1% (v/v) DMSO for 24 h. Cells were washed three times with ice-cold PBS, resuspended in RIPA lysis buffer (P0013B, Beyotime), and incubated on ice for 30 min. Cell debris was removed by centrifugation at 13,000 rpm for 30 min at 4 ˚C. The protein concentration of each supernatant sample was determined with Pierce™ BCA Protein Assay Kit (23225, Thermo Fisher). Equal protein amounts were electrophoresed under non-reducing (Uba3-NEDD8, Ubc12-NEDD8, Cullins-Nedd8, Ubc9-SUMO, Ubc10-Ub and USE1-Ub) or reducing (p27, NRF2, CDT1 and cleaved caspase 3) conditions on SDS-PAGEs and subjected to western blot analysis. All experiment was repeated 3 times.

4.8. Western blot analysis

Protein samples were transferred to a PVDF membrane. The membrane was blocked with 5% (w/v) milk for 1 h at room temperature, and probed with primary antibody diluted (1:1000, v/v) in 5% (w/v) milk overnight at 4 ˚C. The membrane was washed with TBS/0.1% (v/v) Tween 20 (TBST) and incubated with horseradish peroxide-conjugated secondary antibody diluted (1:4000, v/v) in 5% (w/v) milk for 1.5 h at room temperature. Protein bands were detected using SignalFire™ ECL Reagent (6883, Cell Signaling Technology, CST).

In this assay anti-NEDD8 antibody (2745, CST) was used to measure Uba3-NEDD8, Ubc12-NEDD8 and Cullins-NEDD8. Anti-Ubc9 (4918, CST), anti-Ubc10 (A-650, R&D), anti-USE1 (Sc-102150, Santa Cruz), anti-p27 (KF446, Nanjing Jiancheng Bioengineering Institute), anti-CDT1 (8064, CST), anti-NRF2 (12721, CST) and anti-cleaved caspase 3 (9661, CST) antibodies were utilized to recognize Ubc9-Ub, Ubc10-SUMO, USE1-Ub, p27, CDT1, NRF2 and cleaved caspase 3 respectively. Densitometry analysis of the Western blot was conducted by using Image J. All experiment was repeated 3 times.

4.9. Apoptosis/necrosis assay

Apoptosis/necrosis was evaluated using FITC annexin V apoptosis detection kit (556547, BD Biosciences). AGS cells were seeded at 3×10^5 cells per well in 6-well plates and allowed to attach in 12 h. Cells were treated with different concentrations of **LP0040** (0 μM, 4 μM, 6 μM, 8 μM, and 10 μM) for 36 h. Cells were dissociated using trypsin. Dissociated cells were washed twice with cold PBS and resuspended in 100 μL 1× binding buffer, followed by the addition of 5 μL FITC annexin V staining solution and 5 μL PI staining solution. After incubation at room temperature in the dark for 15 min, another 400 μL 1×binding buffer was added. Stained cells were analyzed immediately by flow cytometry (FACSCalibur, BD Biosciences). In each sample 10000 cells were examined, and fluorescence

was measured at an excitation wave length of 488 nm through FL-1 (530 nm) and FL-3 (630 nm) filters.

4.10. Cell cycle assay

AGS cells were seeded at a density of 1×10^5 cells per well in a final volume of 2 mL/well in a six-well plate and left to attach for 24 h at 37 ˚C in a 5% CO_2 incubator. Cells treated with 4 μM **LP0040** for different time were harvested and fixed in 70% ethanol at −20 °C overnight. They were then incubated with PI/RNase staining buffer (550825, BD Biosciences) in the dark for 15–20 min and analyzed by flow cytometry (FACSCalibur, BD Biosciences). In each sample 20000 cells were examined, and fluorescence was measured at an excitation wave length of 488 nm through FL-3 (630 nm) filters. The experiment was repeated 3 times.

4.11. Synergistic effect of LP0040 with bortezomib

AGS cells (6×10^3/well) were plated in 96-well plates. After 12 h for attachment, AGS cells were treated with indicated concentrations of **LP0040**, bortezomib and combination, respectively. Following 48 h incubation, 5 μL CCK-8 was added to each well and cells were incubated for 4 h. The light absorption value (OD) of each well was measured at 450 nm. Inhibition rates were calculated, and the *q* value was calculated according to the equation:

$$q = \frac{\mathrm{E_{LP0040+BTZ}}}{\mathrm{E_{LP0040}} + \mathrm{E_{BTZ}} - \mathrm{E_{LP0040}} \times \mathrm{E_{BTZ}}}$$

Where E_{LP0040}, E_{BTZ} and $E_{LP0040+BTZ}$ are the inhibition rates of **LP0040**, bortezomib, and combination of **LP0040** and bortezomib, respectively.

The experiment was repeated 3 times.

4.12. Hemolysis assay

Hemolysis assay was conducted as the method previously reported[38]. Rabbit erythrocytes were harvested by centrifugation for 10 min at 3000 rpm, washed two times with PBS and finally suspended in PBS for immediate use. Of that suspension, 150 μL was added in 1.5 mL centrifuge tube containing 150 μL of 200 μM tested compounds in the same buffer. 0 and 100% hemolysis was respectively achieved with PBS and 1% Triton X-100. Centrifuge tubes were incubated for 1 h at 37 ˚C and suspensions were centrifuged at 3000 rpm for 5 min. Supernatant were transferred to 96-well plates and hemoglobin release was measured by microplate reader at 540 nm. Hemolytic ratio was calculated according to the equation:

$$\mathrm{Hemolysis\%} = \frac{A_{test} - A_{control}}{A_{TritonX-100} - A_{control}} \times 100\%$$

4.13. Log P measurement

Log P values of **9, 10, 11**, **12**, **15, 16**, **17** and **18** were measured using shake-flask method. Each compound was dissolved in 1 mL water (water was saturated with 1-octanol), and then an equal volume of 1-octanol (1-octanol was saturated with water) was added. The tube was shaken for 24 h at 37 °C to allow the compound to partition to each phase. After being centrifugated at 5000 rpm , compound in each phase was determined by HPLC (LC-20A, SHIMADZU) at 254 nM. All the experiments were carried out in triplicate. The partition coefficient was calculated using the equation below.

$$\text{Log P}=\log_{10}\frac{\text{AUC}_{\text{octanol}}}{\text{AUC}_{\text{water}}}$$

Supporting information. Supplementary data related to this article can be found at https://doi.org/ XXXXXXXXX.

Author information

Corresponding author

* Yubin Wang, School of Pharmaceutical Sciences, Nanjing Tech University, No. 5 Xinmofan Road, Nanjing 210009, People's Republic of China. Tel. +86 25 83172108; Fax: +86 25 83172105; E-mail: wyb5393@njtech.edu.cn.

Conflicts of interest

None of the authors of the above manuscript has declared any conflict of interest which may arise from being named as an author on the manuscript.

Acknowledgements

The authors thank Professor Hai Qian (China Pharmaceutical University, Nanjing, China) for providing the K562 cells. This work was supported by the Natural Science Foundation for Colleges and Universities in Jiangsu Province (No. 11KJB350002), the Natural Science Foundation of Jiangsu Province (No.BK2012422, BK20141015) and the National Natural Science Foundation of China (No. 81202393, 81600159).

Reference

[1] A. Hershko, The ubiquitin system for protein degradation and some of its roles in the control of the cell division cycle, Cell. Death Differ. 12 (2005) 1191-1197.

[2] S.T. Nawrocki, K.R. Kelly, P.G. Smith, C.M. Espitia, A. Possemato, S.A. Beausoleil, M. Milhollen, S. Blakemore, M. Thomas, A. Berger, J.S. Carew, Disrupting Protein NEDDylation with MLN4924 Is a Novel Strategy to Target Cisplatin Resistance in Ovarian Cancer, Clin. Cancer Res. 19 (2013) 3577-3590.

[3] R.C. Kane, P.F. Bross, A.T. Farrell, R. Pazdur, Velcade®: US FDA approval for the treatment of multiple

myeloma progressing on prior therapy, Oncologist 8 (2003) 508-513.

[4] B.K. Boh, P.G. Smith, T. Hagen, Neddylation-Induced Conformational Control Regulates Cullin RING Ligase Activity In Vivo, J. Mol. Biol. 409 (2011) 136-145.

[5] T.A. Soucy, P.G. Smith, M. Rolfe, Targeting NEDD8-Activated Cullin-RING Ligases for the Treatment of Cancer, Clin. Cancer Res. 15 (2009) 3912-3916.

[6] P. Xie, M. Zhang, S. He, K. Lu, Y. Chen, G. Xing, Y. Lu, P. Liu, Y. Li, S. Wang, N. Chai, J. Wu, H. Deng, H.-R. Wang, Y. Cao, F. Zhao, Y. Cui, J. Wang, F. He, L. Zhang, The covalent modifier Nedd8 is critical for the activation of Smurf1 ubiquitin ligase in tumorigenesis, Nat. Commun. 5 (2014) 3733.

[7] D.P. Xirodimas, M.K. Saville, J.-C. Bourdon, R.T. Hay, D.P. Lane, Mdm2-Mediated NEDD8 Conjugation of p53 Inhibits Its Transcriptional Activity, Cell 118 (2004) 83-97.

[8] W.M. Abida, A. Nikolaev, W. Zhao, W. Zhang, W. Gu, FBXO11 Promotes the Neddylation of p53 and Inhibits Its Transcriptional Activity, J. Biol. Chem. 282 (2007) 1797-1804.

[9] N.H. Stickle, J. Chung, J.M. Klco, R.P. Hill, W.G. Kaelin, M. Ohh, pVHL Modification by NEDD8 Is Required for Fibronectin Matrix Assembly and Suppression of Tumor Development, Mol. Cell. Biol. 24 (2004) 3251-3261.

[10] F. Gao, J. Cheng, T. Shi, E.T.H. Yeh, Neddylation of a breast cancer-associated protein recruits a class III histone deacetylase that represses NFκB-dependent transcription, Nat. Cell Biol. 8 (2006) 1171-1177.

[11] M. Fan, R.M. Bigsby, K.P. Nephew, The NEDD8 Pathway Is Required for Proteasome-Mediated Degradation of Human Estrogen Receptor (ER)-α and Essential for the Antiproliferative Activity of ICI 182,780 in ERα-Positive Breast Cancer Cells, Mol. Endocrinol. 17 (2003) 356-365.

[12] T.A. Soucy, P.G. Smith, M.A. Milhollen, A.J. Berger, J.M. Gavin, S. Adhikari, J.E. Brownell, K.E. Burke, D.P. Cardin, S. Critchley, C. A. Cullis, A. Doucette, J. J.Garnsey, J. L. Gaulin, R. E. Gershman, A. R. Lublinsky, A. McDonald, H. Mizutani, U. Narayanan, E. J. Olhacva, S. Peluso, M. Rezaei, M. D. Sintchak, T. Talreja, M. P. Thomas, T. Traore, S. Vyskocil, G. S. Weatherhead, J. Yu, J. Zhang, L. R. Dick, C. F. Claiborne, M. Rolfe, J. B. Bolen, S. P. Langston, An inhibitor of NEDD8-activating enzyme as a new approach to treat cancer, Nature 458 (2009) 732-736.

[13] L. Li, M. Wang, G. Yu, P. Chen, H. Li, D. Wei, J. Zhu, L. Xie, H. Jia, J. Shi, C. Li, W. Yao, Y. Wang, Q. Gao, L.S. Jeong, H.W. Lee, J. Yu, F. Hu, J. Mei, P. Wang, Y. Chu, H. Qi, M. Yang, Z. Dong, Y. Sun, R.M. Hoffman, L. Jia, Overactivated Neddylation Pathway as a Therapeutic Target in Lung Cancer, J. Natl. Cancer Inst. 106 (2014) dju083.

[14] Q. Gao, G.-Y. Yu, J.-Y. Shi, L.-H. Li, W.-J. Zhang, Z.-C. Wang, L.-X. Yang, M. Duan, H. Zhao, X.-Y. Wang, J. Zhou, S.-J. Qiu, L.S. Jeong, L.-J. Jia, J. Fan, Neddylation pathway is up-regulated in human intrahepatic cholangiocarcinoma and serves as a potential therapeutic target, Oncotarget 5 (2014) 7820-7832.

[15] J.J. Lin, M.A. Milhollen, P.G. Smith, U. Narayanan, A. Dutta, NEDD8-Targeting Drug MLN4924 Elicits DNA Rereplication by Stabilizing Cdt1 in S Phase, Triggering Checkpoint Activation, Apoptosis, and Senescence in Cancer Cells, Cancer Res. 70 (2010) 10310-10320.

[16] J.I. Toth, L. Yang, R. Dahl, M. D. Petroski, A Gatekeeper Residue for NEDD8-Activating Enzyme Inhibition by MLN4924, Cell Rep. 1 (2012) 309-316.

[17]M.A. Milhollen, M.P. Thomas, U. Narayanan, T. Traore, J. Riceberg, B.S. Amidon, N.F. Bence, J.B. Bolen, J. Brownell, L.R. Dick, H.-K. Loke, A.A. McDonald, J. Ma, M. G. Manfredi, T. B. Sells, M. D. Sintchak, X. Yang, Q. Xu, E. M. Koenig, J. M. Gavin, P. G. Smith, Treatment-Emergent Mutations in NAE² Confer Resistance to the NEDD8-Activating Enzyme Inhibitor MLN4924, Cancer cell 21 (2012) 388-401.

[18] G.W. Xu, J.I. Toth, S.R. da Silva, S.-L. Paiva, J.L. Lukkarila, R. Hurren, N. Maclean, M.A. Sukhai, R.N. Bhattacharjee, C.A. Goard, P.T. Gunning, S. Dhe-Paganon, M.D. Petroski, A.D. Schimmer, Mutations in UBA3 Confer Resistance to the NEDD8-Activating Enzyme Inhibitor MLN4924 in Human Leukemic Cells, PLoS One 9 (2014) e93530.

[19] C.-H. Leung, D.S.-H. Chan, H. Yang, R. Abagyan, S.M.-Y. Lee, G.-Y. Zhu, W.-F. Fong, D.-L. Ma, A natural product-like inhibitor of NEDD8-activating enzyme, Chem. Commun. 47 (2011) 2511-2513.

[20] H.-J. Zhong, V. Pui-Yan Ma, Z. Cheng, D. Shiu-Hin Chan, H.-Z. He, K.-H. Leung, D.-L. Ma, C.-H. Leung, Discovery of a natural product inhibitor targeting protein neddylation by structure-based virtual screening, Biochimie 94 (2012) 2457-2460.

[21] H.-J. Zhong, H. Yang, D.S.-H. Chan, C.-H. Leung, H.-M. Wang, D.-L. Ma, A Metal-Based Inhibitor of NEDD8-Activating Enzyme, PLoS One 7 (2012) e49574.

[22] S. Zhang, J. Tan, Z. Lai, Y. Li, J. Pang, J. Xiao, Z. Huang, Y. Zhang, H. Ji, Y. Lai, Effective Virtual Screening Strategy toward Covalent Ligands: Identification of Novel NEDD8-Activating Enzyme Inhibitors, J. Chem. Inf. Model. 54 (2014) 1785-1797.

[23] H. An, A.V. Statsyuk, An inhibitor of ubiquitin conjugation and aggresome formation, Chem. Sci. 6 (2015) 5235-5245.

[24] H. Ma, C. Zhuang, X. Xu, J. Li, J. Wang, X. Min, W. Zhang, H. Zhang, Z. Miao, Discovery of benzothiazole derivatives as novel non-sulfamide NEDD8 activating enzyme inhibitors by target-based virtual screening, Eur. J. Med. Chem. 133 (2017) 174-183.

[25] K.-J. Wu, H.-J. Zhong, G. Li, C. Liu, H.-M.D. Wang, D.-L. Ma, C.-H. Leung, Structure-based identification of a NEDD8-activating enzyme inhibitor via drug repurposing, Eur. J. Med. Chem. 143 (2018) 1021-1027.

[26] P. Lu, X. Liu, X. Yuan, M. He, Y. Wang, Q. Zhang, P.-k. Ouyang, Discovery of a novel NEDD8 Activating Enzyme Inhibitor with Piperidin-4-amine Scaffold by Structure-Based Virtual Screening, ACS Chem. Biol. 11 (2016) 1901-1907.

[27] S. Bellon, J.D. Parsons, Y. Wei, K. Hayakawa, L.L. Swenson, P.S. Charifson, J.A. Lippke, R. Aldape, C.H. Gross, Crystal Structures of Escherichia coli Topoisomerase IV ParE Subunit (24 and 43 Kilodaltons): a Single Residue Dictates Differences in Novobiocin Potency against Topoisomerase IV and DNA Gyrase, Antimicrob. Agents Ch. 48 (2004) 1856-1864.

[28] D. Lafitte, V. Lamour, P.O. Tsvetkov, A.A. Makarov, M. Klich, P. Deprez, D. Moras, C. Briand, R. Gilli, DNA Gyrase Interaction with Coumarin-Based Inhibitors: The Role of the Hydroxybenzoate Isopentenyl Moiety and the 5′-Methyl Group of the Noviose, Biochemistry 41 (2002) 7217-7223.

[29] C. Luca, B. Daniela, Privileged Structures as Leads in Medicinal Chemistry, Curr. Med. Chem. 13 (2006) 65-85.

[30] J.L. Lukkarila, S.R. da Silva, M. Ali, V.M. Shahani, G.W. Xu, J. Berman, A. Roughton, S. Dhe-Paganon, A.D. Schimmer, P.T. Gunning, Identification of NAE Inhibitors Exhibiting Potent Activity in Leukemia Cells: Exploring the Structural Determinants of NAE Specificity, ACS Med. Chem. Lett. 2 (2011) 577-582.

[31] L. Tan, X.e. Jia, X. Jiang, Y. Zhang, H. Tang, S. Yao, Q. Xie, In vitro study on the individual and synergistic cytotoxicity of adriamycin and selenium nanoparticles against Bel7402 cells with a quartz crystal microbalance, Biosens. Bioelectron. 24 (2009) 2268-2272.

[32] Z.-J. JIN, About the evaluation of drug combination, Acta Pharmacol. Sin. 25 (2004) 146-147.

[33] M. Lin, J. Hou, W. Chen, X. Huang, Z. Liu, Y. Zhou, Y. Li, T. Zhao, L. Wang, K.-W. Wu, Z. Shen, Improved Response Rates with Bortezomib in Relapsed or Refractory Multiple Myeloma: An

Observational Study in Chinese Patients, Adv. Ther. 31 (2014) 1082-1094.

[34] J.R. Mikhael, A.R. Belch, H.M. Prince, M.N. Lucio, A. Maiolino, A. Corso, M.T. Petrucci, P. Musto, M. Komarnicki, A.K. Stewart, High response rate to bortezomib with or without dexamethasone in patients with relapsed or refractory multiple myeloma: results of a global phase 3b expanded access program, Brit. J. Haematol. 144 (2009) 169-175.

[35] P.G. Richardson , B. Barlogie , J. Berenson , S. Singhal , S. Jagannath , D. Irwin , S.V. Rajkumar , G. Srkalovic , M. Alsina , R. Alexanian , D. Siegel , R.Z. Orlowski , D. Kuter , S.A. Limentani , S. Lee , T. Hideshima , D.-L. Esseltine , M. Kauffman , J. Adams , D.P. Schenkein , K.C. Anderson A Phase 2 Study of Bortezomib in Relapsed, Refractory Myeloma, New England J. Med. 348 (2003) 2609-2617.

[36] H. Tanaka, E. Kono, C.P. Tran, H. Miyazaki, J. Yamashiro, T. Shimomura, L. Fazli, R. Wada, J. Huang, R.L. Vessella, J. An, S. Horvath, M. Gleave, M.B. Rettig, Z.A. Wainberg, R.E. Reiter, Monoclonal antibody targeting of N-cadherin inhibits prostate cancer growth, metastasis and castration resistance, Nat. Med. 16 (2010) 1414-1420.

[37] J. Ding, S. Huang, S. Wu, Y. Zhao, L. Liang, M. Yan, C. Ge, J. Yao, T. Chen, D. Wan, H. Wang, J. Gu, M. Yao, J. Li, H. Tu, X. He, Gain of miR-151 on chromosome 8q24.3 facilitates tumour cell migration and spreading through downregulating RhoGDIA, Nat. Cell Biol. 12 (2010) 390-399.

[38] S. Yadav, S. Joshi, M. Q. Pasha, S. Pasha, Antimicrobial activity and mode of action of novel, N-terminal tagged tetra-peptidomimetics, MedChemComm 4 (2013) 874-880.

Table 1. IC_{50} values of tested compounds (μM, n=3)

Cell line	A549	AGS	K562	HCT-116	BxPC-3	SKOV-3
9	3.77 ± 0.67	1.89 ±0.27	3.26 ± 0.64	5.82 ± 2.40	8.44 ± 1.47	6.42 ± 0.48
10	3.09 ± 0.99	1.39 ± 0.35	3.29 ± 0.78	6.00 ± 0.90	7.67 ± 1.56	5.94 ± 0.99
11	2.14 ± 0.37	0.76 ± 1.26	2.45 ± 0.31	1.33 ± 0.13	2.80 ± 0.20	3.29 ± 1.28
12	3.83 ± 0.88	1.26 ± 0.17	1.53 ± 0.39	6.11 ± 0.23	2.82 ± 0.37	3.22 ± 0.13
13	> 30	> 30	> 30	> 30	> 30	> 30
14	> 30	> 30	> 30	> 30	> 30	> 30
15	2.99 ± 0.41	1.13 ± 0.32	1.17 ± 0.18	2.81 ± 0.33	4.08 ± 1.26	4.17 ± 0.29
16	3.10 ± 1.12	1.42 ± 0.17	1.32 ± 0.32	4.27 ± 1.01	1.33 ± 0.24	7.50 ± 1.66
17	3.35 ± 0.79	1.66 ± 0.15	3.30 ± 1.01	2.69 ± 0.28	4.33 ± 1.25	7.70 ± 0.42
18	2.48 ± 0.27	1.71 ± 1.17	2.63 ± 0.26	2.79 ± 1.00	2.01 ± 0.25	4.35 ± 0.19
M22	5.55 ± 0.17	9.92 ± 0.91	5.51 ±1.18	10.57 ± 1.84	12.40 ± 3.68	9.26 ± 1.11

Table 2. LC_{50} values of **LP0040**, MLN4924 and bortezomib against normal cells (μM, n=3)

Cells	HEK293T	HUVEC	L-02
LP0040(11)	12.93 ± 1.09	10.69 ± 0.83	13.54 ± 2.37
MLN4924	6.17 ± 0.44	4.79 ± 0.27	9.01 ± 0.98
BTZ	0.016 ± 0.003	0.018 ± 0.002	0.398 ± 0.041

Table 3. Percentage inhibition values of kinase activity by LP0040 (30 μM)

Kinase	% inhibition
PKAα	5.17 ± 0.49
PKCα	11.49 ± 1.27
Aur A	6.03 ± 0.77
B-raf	1.75 ± 0.26
CDK1	-1.18 ± 0.21
CDK2E	4.57 ± 0.39
CHK1	1.01 ± 0.14
CHK2	9.44 ± 1.44
LCK	-2.51 ± 0.53
PLK	5.58 ± 0.48
AKT	9.87 ± 1.21
EGFR	2.77 ± 0.37
IKKb	1.07 ± 0.14

Table 4. q values for each combination of BTZ and LP0040

BTZ (nM)	LP0040 (μM)		
	1	**1.25**	**1.5**
5	0	4.34**	1.15
7.5	1.13	3.1**	1.05
10	1.14	1.75*	1.35*

** apparent synergism； * synergism

Figure Legends

Fig. 1 overview of the UPS

Fig. 2 Structures of reported NAE inhibitors.

Fig. 3 Scaffold replacement of **M22**: (A) design of compound 8; (B) low-energy binding conformations of **8** bound to NAE heterodimer generated by AutoDock 4. APPBP1-UBA3-NEDD8-ATP complex (PDB ID: 1R4N) was used in docking study (red dashed: H-bond; yellow line: π-cation interaction); (C) merging between top-ranked **8** pose (shown in blue) and ATP conformation (shown in red) from APPBP1-UBA3-NEDD8-ATP complex (PDB ID:1R4N).

Fig. 4 Structures, Log P and hemolysis rate of 7-(4-(phenethylamino) piperidin-1-yl)-2H-chromen-2-one based NAE inhibitors. (A) Structures of designed NAE inhibitors; (B) hemolysis of designed NAE inhibitors (* hemolysis rate < 10%, n=3); (C) Log P of designed NAE inhibitors (n=3).

Fig. 5 Compound **LP0040** was an NAE and UAE dual inhibitor: (A) **LP0040** inhibited NAE and UAE activities in enzyme-based assay; (B) **LP0040** could inhibited neddylation and CRL substrate degradation in AGS cells; (C) selectivity of compound **LP0040** in AGS cells; (D) compound **13** could not inhibit NAE activity in AGS cells.

Fig. 6 Apoptosis induced by **LP0040** in AGS cells. The ratio of apoptotic cells (Annexin V^{+} cells) increased from about 6% to more than 80% with concentration of **LP0040** increasing from 0 μM to 10 μM.

Fig. 7 Cell-based activity evaluation of **LP0040**: (A) cell cycle analysis through flow cytometry (n=3); (B) cell cycle statistics of AGS cells treated with **LP0040**; (C) synergistic effect between **LP0040** and Bortezomib against AGS cells. Inhibition efficiency of drug alone and drug combination on 6×10^3 AGS cells' growth at 48 h after drug introduction. Results are presented as mean ± SD (error bar) of triplicate experiments. Symbols "*" and "**" represent the grades of synergism and apparent synergism, respectively, for evaluating effect of drug combination.

Fig.1

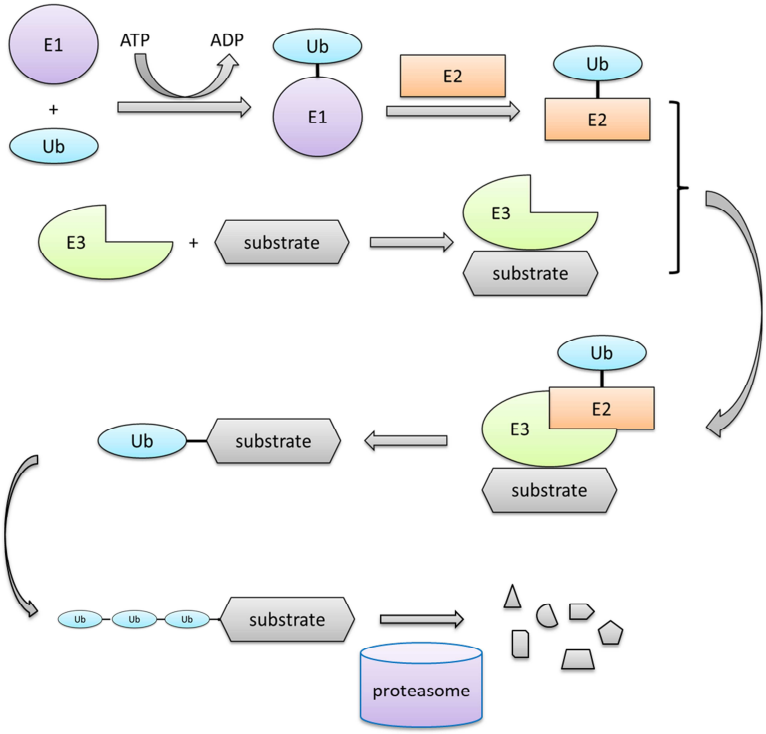

Fig. 2

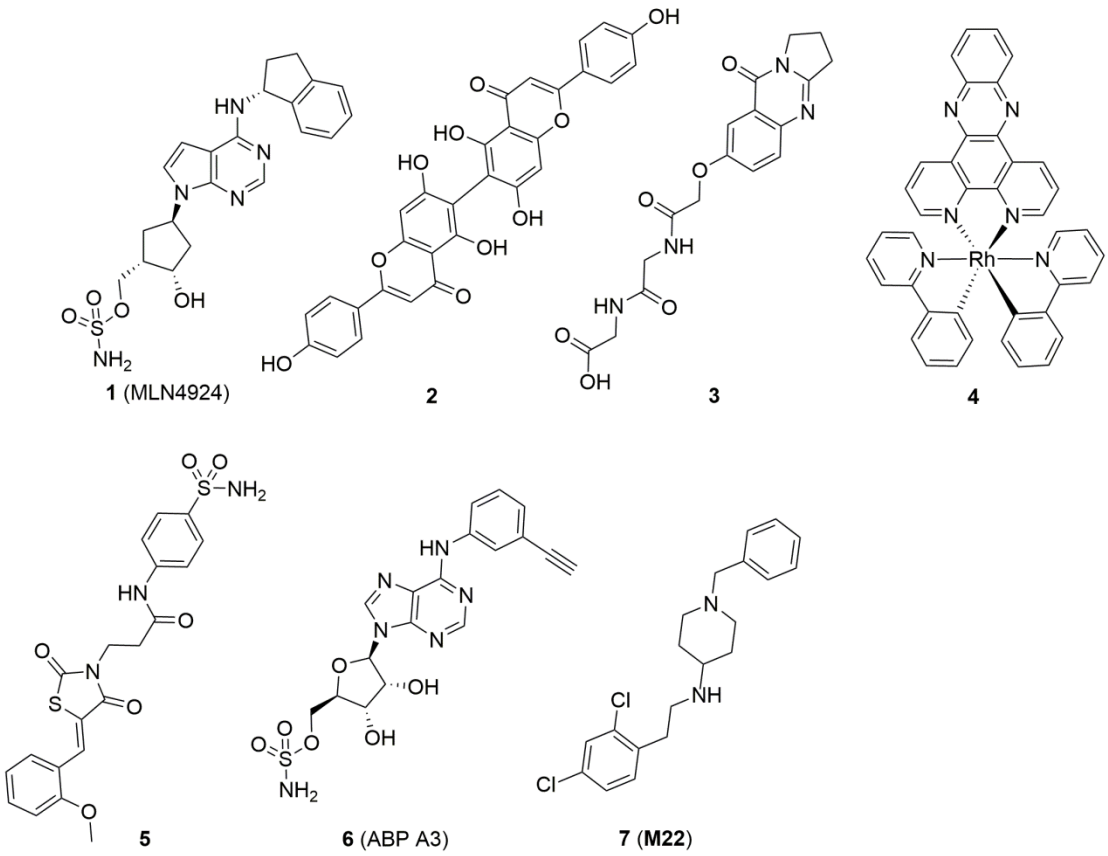

Fig. 3

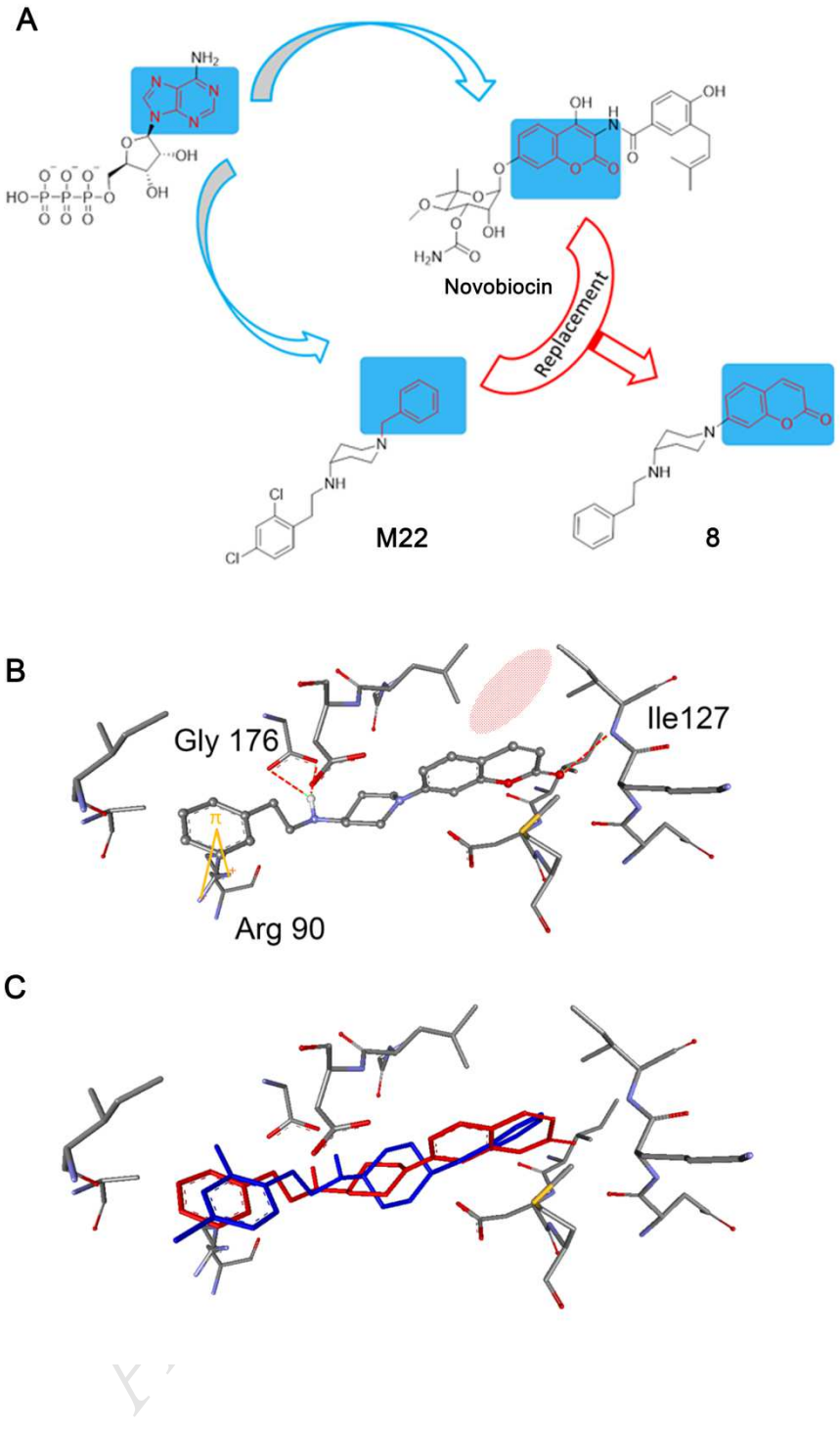

Fig. 4

A

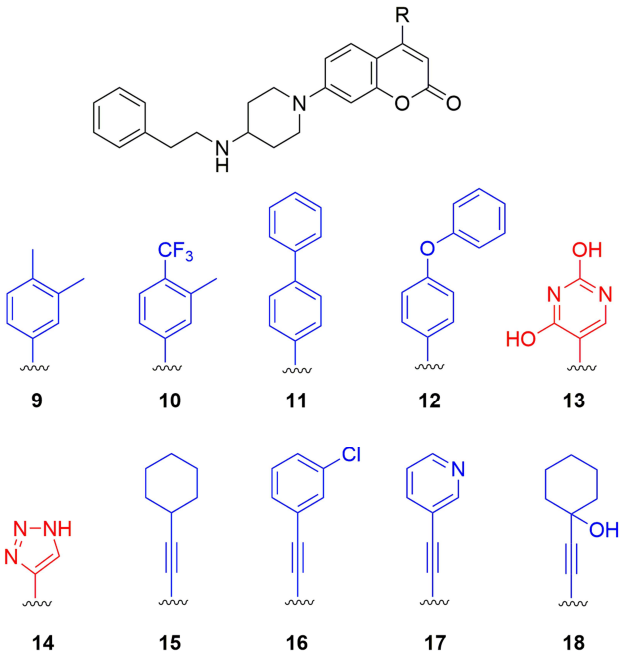
R
N
O
O
N
H
CF3
OH
N
N
HO
9
10
11
12
13
N–NH
N
Cl
N
OH
14
15
16
17
18

B

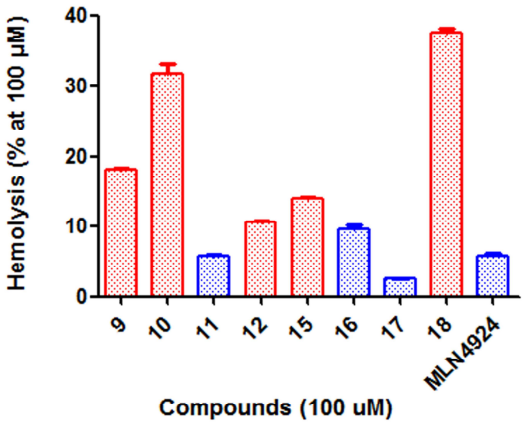
Hemolysis (% at 100 μM)
40
30
20
10
0
9
10
11
12
15
16
17
18
MLN4924
Compounds (100 uM)

C

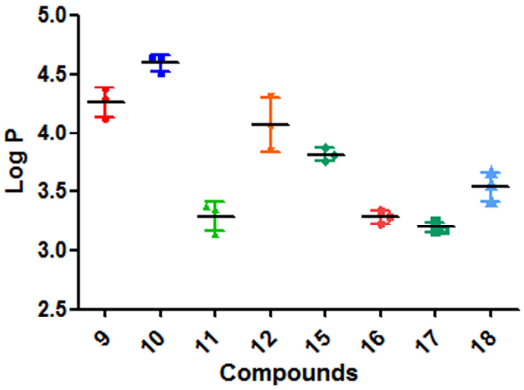
Log P
5.0
4.5
4.0
3.5
3.0
2.5
9
10
11
12
15
16
17
18
Compounds

Fig.5

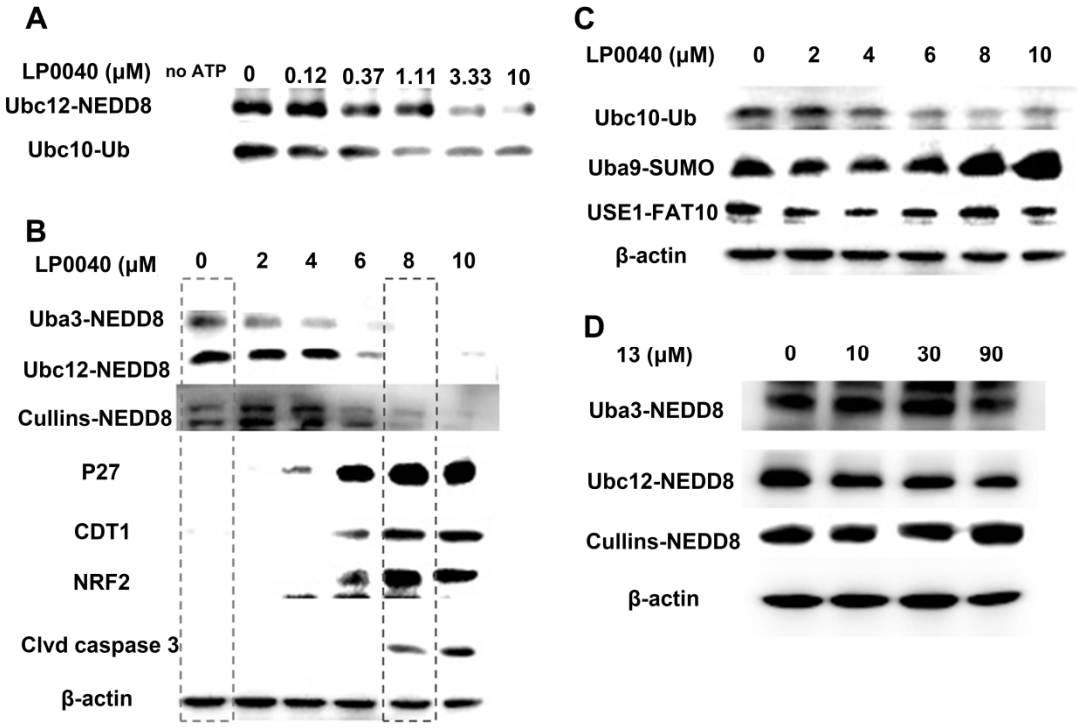

Fig.6

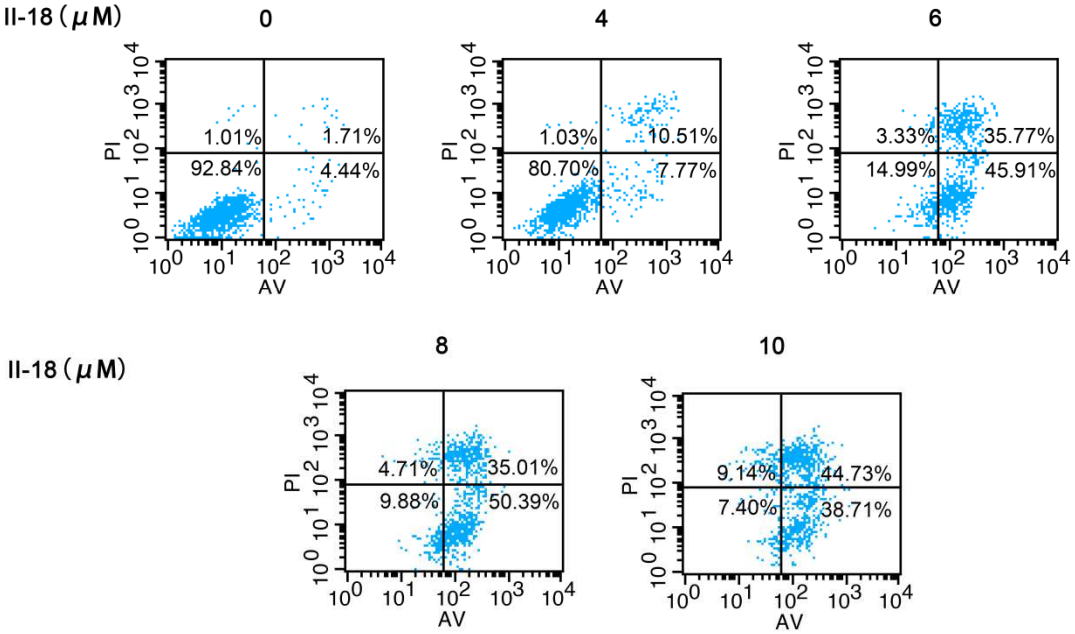

Fig.7

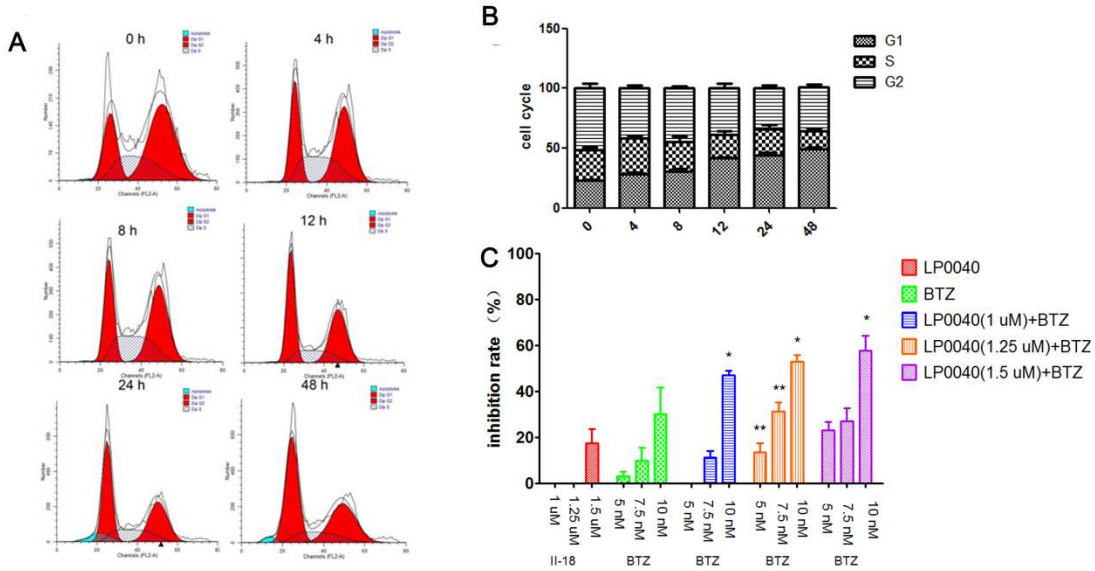

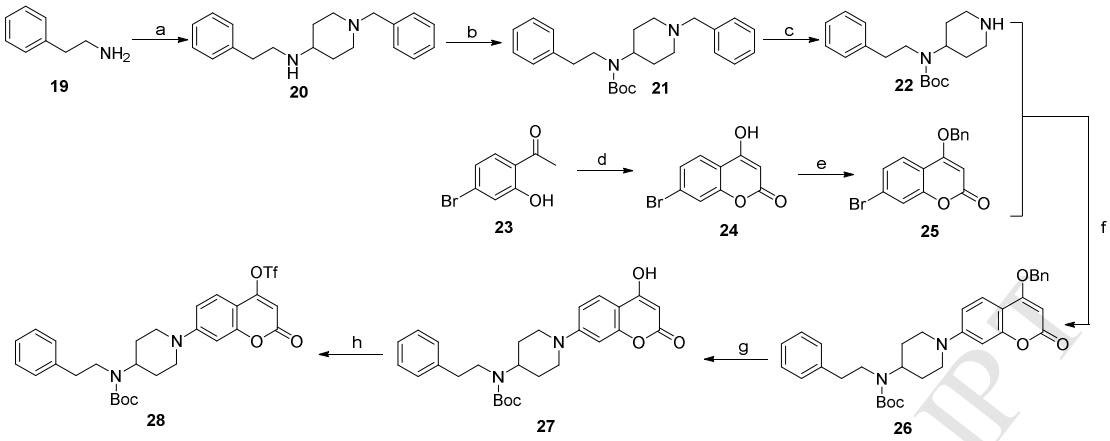

Conditions and reagents: (a) N-Benzyl-4-piperidone, $NaBH_3CN$, MeOH, AcOH, 3h, 0 ˚C, 98.2%; (b) Boc_2O, NaOH, t-BuOH, H_2O, rt, overnight, 77.9%; (c) Pd/C. EtOH, 40 ˚C, overnight, 95.9%; (d) NaH, Dimethyl carbonate, toluene, reflux, 23 h, 92.6%; (e) BnBr, Na_2CO_3, MeCN, reflux, 6h, 62.3%; (f) BINAP, $PdCl_2$, Cs_2CO_3, 1,4-Dioxane, 90 ˚C, overnight, 59.5%; (g) Pd/C, THF, rt, 10 h, 92.6%; (h) Et_3N, $(TfO)_2O$, DCM, rt, 6 h, 62.3%.

Scheme 1 The synthesis method of key intermediate **28**.

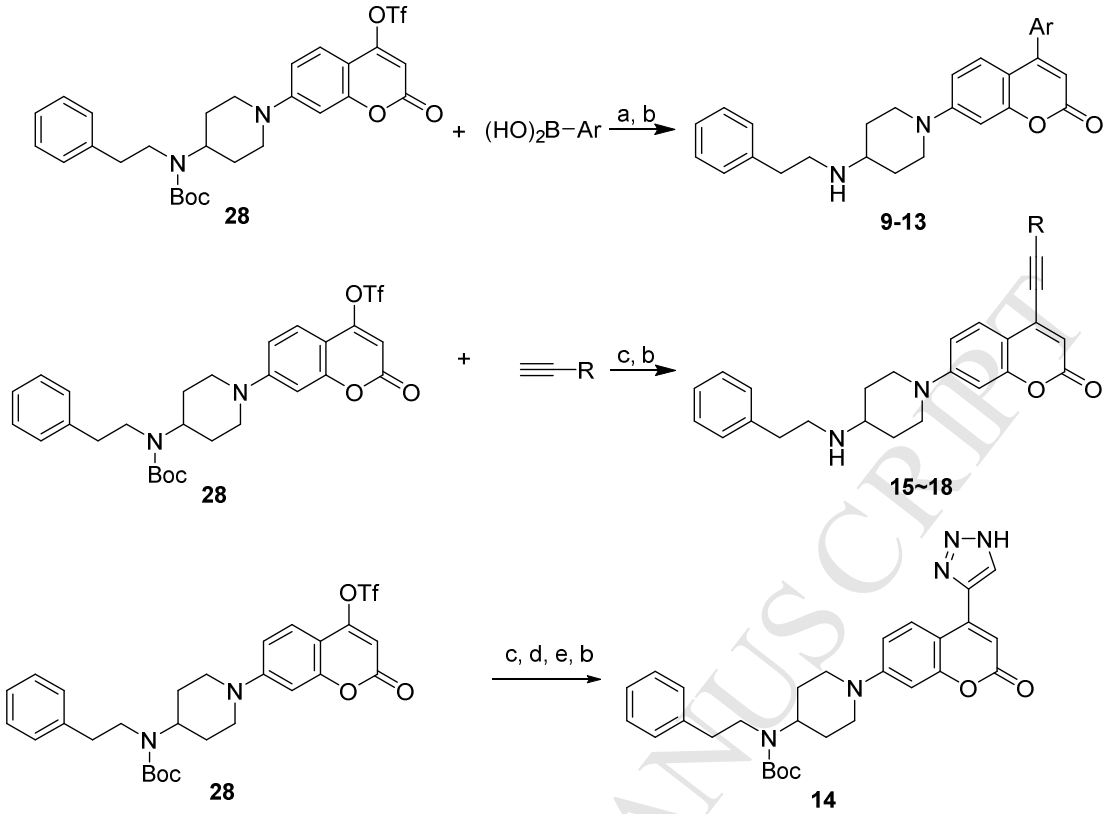

Regents and conditions: (a) BINAP, $PdCl_2$, Cs_2CO_3, 1,4-Dioxane, 90 ˚C, overnight; (b) TFA, DCM, rt, 3 h; (c) Trimethylsilylacetylene, MeCN, $Pd(PPh_3)_4$, CuI, DIPEA, reflux, 3h; (d) NaN_3， DMSO， reflux, 3h; (e) TBAF, DCM, rt, 10 min.

Scheme 2 The synthesis method of target compounds.

Highlights

- A series of 2H-chromen-2-one based molecules were designed and synthesized.
- Novel chemotypes of NAE inhibitors.
- LP0040 which induced cancer cell apoptosis was proposed as an NAE/UAE dual inhibitor.